Supplement to "Multi-scale model of *Mycobacterium tuberculosis* infection maps metabolite and gene perturbations to predict granuloma sterilization"

Elsje Pienaar[1,2], Will Matern[3], Jennifer Linderman[1], Joel S. Bader[3], Denise Kirschner[2]

[1]Department of Chemical Engineering, University of Michigan, Ann Arbor, Michigan, USA, [2]Department of Microbiology and Immunology, University of Michigan Medical School, Ann Arbor, MI, USA, [3]Department of Biomedical Engineering and High-Throughput Biology Center, Johns Hopkins University, Baltimore, MD, USA.

GranSim parameter values

GranSim (is calibrated to NHP data (1-4) and validated by predicting granuloma level outcomes of TNFa, IL10 and IFN knockouts (5-11). Host parameter values for *GranSim* are given in Table S1 (see Table 3 in the main text for bacterial growth parameters specific to this work).

Table S1: *GranSim* parameters

Parameter	Unit*	Baseline Value
Number of host cell deaths causing caseation		10
Time to heal caseation	Days	2298
TNF threshold for causing apoptosis	Molecules	2050
Rate of TNF induced apoptosis	s^{-1}	$1.3x10^{-6}$
Minimum chemokine concentration allowing chemotaxis	Molecules	1
Maximum chemokine concentration allowing chemotaxis	Molecules	400
Initial macrophage density	Fraction of grid comp.	0.0105
Time steps before a resting macrophage can move	Timesteps	2
Time steps before an activated macrophage can move	Timesteps	14
Time steps before an infected macrophage can move	Timesteps	144

TNF threshold for activating NFkB	Molecules	95
Rate of TNF induced NFkB activation	s^{-1}	$1x10^{-5}$
Number of bacteria resting macrophage can phagocytose	Bacteria	1
Probability of resting macrophage killing bacteria		0.25
Adjustment for killing probability of resting macrophages with NFkB activated		0.4
Number of extracellular bacteria that can activate NFkB	Bacteria	200
Threshold for intracellular bacteria causing chronically infected macrophages	Bacteria	10
Threshold for intracellular bacteria causing macrophage to burst	Bacteria	15
Number of bacteria activated macrophage can phagocytose	Bacteria	5
Probability of an activated macrophage healing a caseated compartment in its Moore neighborhood		0.014
Probability of a T-cell moving to the same compartment as a macrophage		0.07
IFN γ -producing T-cell probability of inducing Fas/FasL mediated apoptosis		0.02
IFN γ -producing T-cell probability of producing TNF		0.07
IFN γ -producing T-cell probability of producing IFN		0.35
Cytotoxic T-cell probability of killing a macrophage		0.01
Cytotoxic T-cell probability of killing a macrophage and all of its intracellular bacteria		0.75
Cytotoxic T-cell probability of producing TNF		0.07
Regulatory T-cell probability of deactivating activated macrophage		0.015
Time before maximum recruitment rates are reached	Timesteps*	720
Macrophage maximal recruitment probability		0.2

Macrophage chemokine recruitment threshold	Molecules	0.151
Macrophage TNF recruitment threshold	Molecules	0.05
Macrophage half sat for TNF recruitment	Molecules	0.55
Macrophage half sat for chemokine recruitment	Molecules	5
IFN γ -producing T-cell maximal recruitment probability		0.096
IFN γ -producing T-cell chemokine recruitment threshold	Molecules	0.151
IFN γ -producing T-cell TNF recruitment threshold	Molecules	0.1
IFN γ -producing T-cell half sat for TNF recruitment	Molecules	0.4
IFN γ -producing T-cell half sat for chemokine recruitment	Molecules	1.5
Cytotoxic T-cell maximal recruitment probability		0.08
Cytotoxic T-cell chemokine recruitment threshold	Molecules	0.3775
Cytotoxic T-cell TNF recruitment threshold	Molecules	0.1
Cytotoxic T-cell half sat for TNF recruitment	Molecules	0.4
Cytotoxic T-cell half sat for chemokine recruitment	Molecules	1.5
Regulatory T-cell maximal recruitment probability		0.024
Regulatory T-cell chemokine recruitment threshold	Molecules	0.0755
Regulatory T-cell TNF recruitment threshold	Molecules	0.1
Regulatory T-cell half sat for TNF recruitment	Molecules	0.4
Regulatory T-cell half sat for chemokine recruitment	Molecules	1.5

*Conversion factor: 10 min/timestep.

Qualitative comparison between GSMN-TB with sMtb

To determine the robustness of our results with respect to our choice of bacterial metabolic model we compare GSMN-TB with sMtb, which merges the metabolic models GSMN-TB(12), iNJ661(13), and MAP (14). To measure the agreement between the models we focus on the reduction in growth rate due to bacterial gene knockouts with different carbon sources (glucose only, lipid only, and glucose + lipid) and with or without hypoxia (defined as a 90% reduction in the permitted oxygen use rate). For both models we use the same rate parameters and nutrient availabilities as were used in *GranSim-CBM*. There are 759 genes associated with reactions in GSMN-TB, 915 genes in sMtb, and 737 in the intersection. We compute the growth rates predicted by both models, with and without the reactions corresponding to each gene in the intersection (single KOs only). The Pearson correlation coefficient for the KO growth rates predicted by sMtb and GSMN-TB ranged from .750 to .797 under the 6 different nutrient conditions we tested. Cross-tabulations of mutants with full growth (defined as >99% of WT), slow growth (0.1% to 99% of WT), and no growth (<0.1% of WT) in each model are provided (Table S2).

Table S2: Cross-tabulations of mutants in GSMN-TB vs sMtb.

Lipid-only_hypoxic	sMtb-full growth	sMtb-slow growth	sMtb-no growth
GSMN-full growth	383	6	26
GSMN-slow growth	4	6	24
GSMN-no growth	43	6	239

Glucose-only_hypoxic	sMtb-full growth	sMtb-slow growth	sMtb-no growth
GSMN-full growth	381	7	26
GSMN-slow growth	12	18	10
GSMN-no growth	36	15	232

Rich_hypoxic	sMtb-full growth	sMtb-slow growth	sMtb-no growth
GSMN-full growth	381	7	26
GSMN-slow growth	12	21	10
GSMN-no growth	36	12	232

Lipid-only_High O2	sMtb-full growth	sMtb-slow growth	sMtb-no growth
GSMN-full growth	378	6	22
GSMN-slow growth	8	2	24
GSMN-no growth	46	5	246

Glucose-only_High O2	sMtb-full growth	sMtb-slow growth	sMtb-no growth
GSMN-full growth	383	5	22
GSMN-slow growth	12	18	10
GSMN-no growth	36	15	236

Rich_High O2	sMtb-full growth	sMtb-slow growth	sMtb-no growth
GSMN-full growth	383	5	22
GSMN-slow growth	12	21	10
GSMN-no growth	36	12	236

Mechanics of bacterial agents in *GranSim-FBM*

A description of the mechanics of bacterial agents in GranSim-FBM is shown in Figure S1 and is summarized as follows:

1) Based on current concentrations of extracellular nutrients and mass of internal lipid deposits, compute upper bounds for constrained reactions. Scale the upper bounds by the current mass of the bacterium.
2) Solve the linear programming problem.
3) Using certain elements of v (the growth rate and the lipid inclusion accumulation and use rates) update the cumulative biomass and lipid inclusion levels.
4) Subtract utilized nutrients from the local extracellular nutrients.
5) Check if lipid inclusion levels exceed limit, if so then reduce levels to maximum.
6) If biomass exceeds 2 then divide, if less than .5 remove the agent.
7) Repeat for each bacterium.

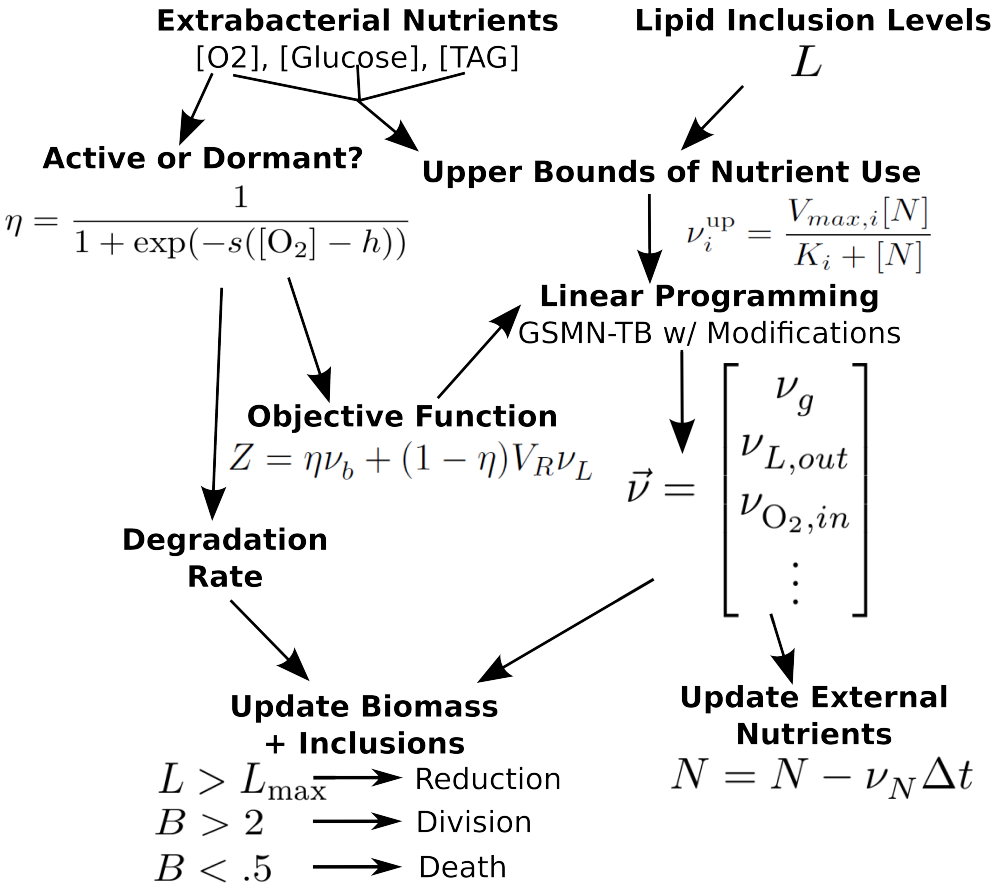

Figure S1: Schematic showing the computation of bacterial growth and response to environmental nutrients.

In silico* knockouts of TNFα , IL-10 and IFNγ in *GranSim

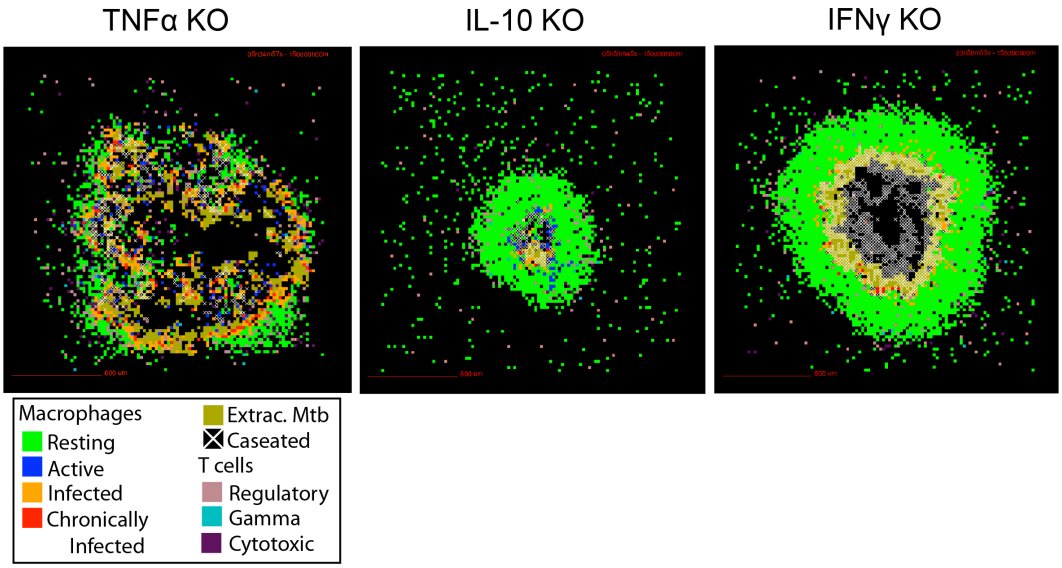

Figure S2: Representative outcomes of *GranSim* 150 days post infection when TNFα , IL-10 or IFNγ are removed from the onset of infection. Outcomes correspond to tissue scale outcomes of TNFα (poor granuloma structure, high bacterial loads), IL-10 (lower bacterial loads, increased inflammation) and IFNγ knockouts (high bacterial loads, tissue damage (caseation)) in mice and NHPs (5-11).

Bacterial growth phenotypes in granulomas are dynamic and heterogeneous

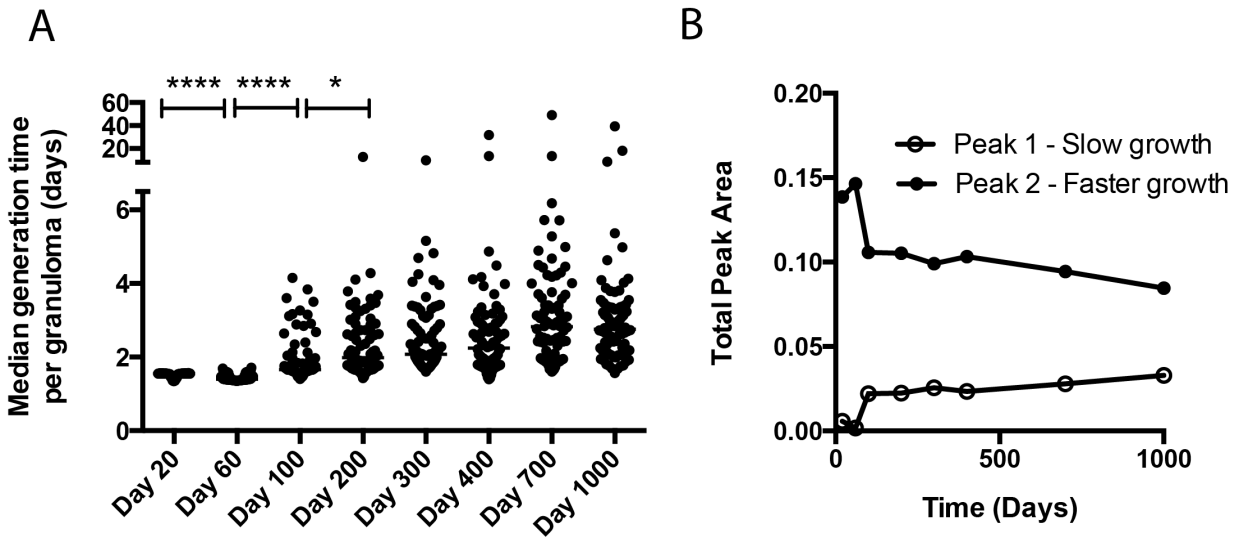

Figure S3: Despite a trend toward slower bacterial growth, the majority of bacteria remain in the faster growth phenotype. (A) Each point represents one granuloma. The y-axis shows the median generation time for each granuloma. Significance: *: $p < 0.01$, ****: $p < 0.00001$ for paired one way ANOVA with Holm-Sidak correction for multiple comparisons. (B) Total area under two peaks in Figure 4B of the main text. Peak 1 represents slow growing Mtb with growth rates < 0.0015 hr^{-1}. Peak 2 represent faster growing Mtb with growth rates ~0.033 hr^{-1}.

Growth phenotype changes reflect granuloma size and bacterial loads

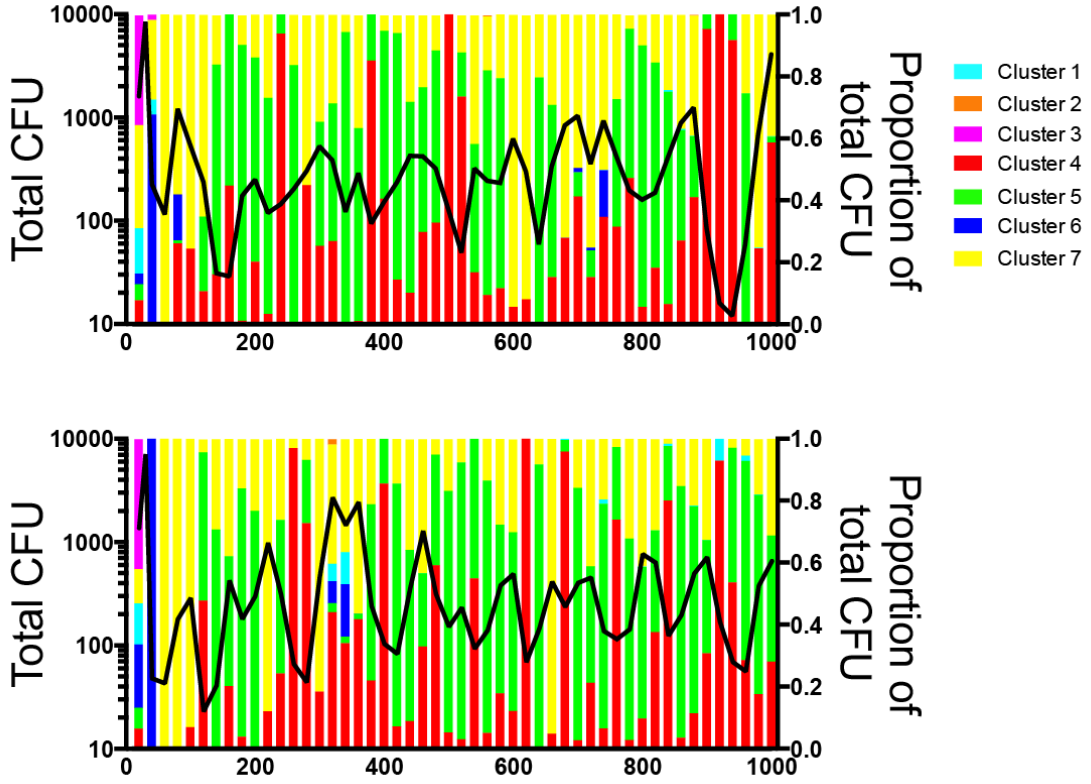

Figure S4: Bacterial growth phenotype changes with time and reflects bacterial load. Two representative granulomas generated by stochastic variation using the same parameters as in Figure 6A in the main text. Proportions of bacteria in each growth cluster (7 clusters identified in Figure 5 of the main text) are quantified every 20 days over the course of infection (right y-axis) and plotted with total CFU (left y-axis).

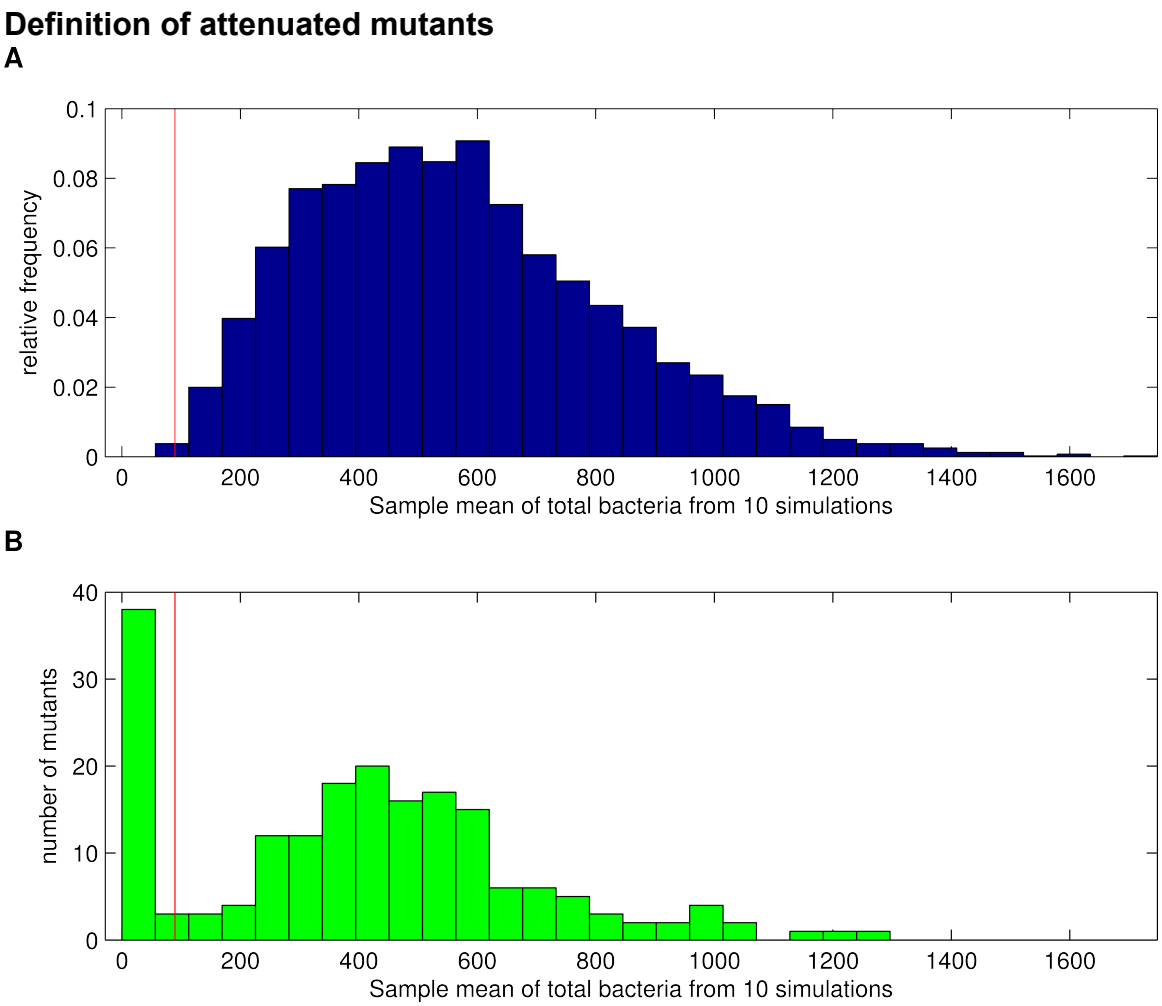

Figure S5: **Defining attenuated knockout mutants.** (A) Histogram showing the distribution of average predicted bacterial loads 400 dpi for WT simulations. The "null" distribution was generated from 4000 bootstrapped samples from 100 ABM-CBM simulations. Red line indicates threshold below which we define an attenuated mutant. The threshold was determined by controlling expected false discoveries. We set alpha such that the expected number of false discoveries from the 191 mutants we tested was less than 1 assuming each mutant followed the null distribution. (B) Histogram showing the distribution of average predicted bacterial loads 400 dpi for 191 Mtb knockouts. Red line indicates the boundary below which we can define attenuated mutants. 41 knockouts fall into this category.

List of attenuated mutants

Table S3.
Mutants attenuated for growth as identified by hypothesis testing using the output from *GranSim-FBM*. Note that Table 5 is the same list but the mutants unable to grow with lipids as the only carbon source have been removed for clarity. All of the mutants unable to grow in lipid only conditions were identified as attenuated by hypothesis testing on the *GranSim-FBM* output.

Gene removed from the reaction set in each KO mutant				**Import rates during optimal growth (fmol/h-BU)**	
Name	**Enzymatic Activity**	**Reaction catalyzed**	**Optimal rate of biomass production (1/h)**	**TAG**	**Oxygen**
WT	N/A	NA	0.034	0.003	0.272
tpi/Rv1438	triose-phosphate isomerase	DHAP <=> G3P	0.023	0.005	0.272
sdhC/Rv3316, sdhB/Rv3319, sdhD/Rv3317, sdhA/Rv3318	succinate dehydrogenase, sdhABCD	MK + SUCC <=> MKH2 + FUM	0	NA	NA
pgk/Rv1437	phosphoglycerate kinase	ADP + 13PDG <=> ATP + 3PG	0.013	0.007	0.272
pgi/Rv0946c	glucose-6-phosphate isomerase, glucose-6-phosphate isomerase-pgi	G6P <=> bDG6P , G6P <=> F6P	0	NA	NA
otsB2/Rv3372	trehalose-phosphatase otsB2	TRE6P -> PI + TRE	0	NA	NA

nuoA/Rv3145, nuoB/Rv3146, nuoD/Rv3148, nuoE/Rv3149, nuoF/Rv3150, nuoG/Rv3151, nuoH/Rv3152, nuoI/Rv3153, nuoJ/Rv3154, nuoK/Rv3155, nuoL/Rv3156, nuoM/Rv3157, nuoN/Rv3158	type I NADH dehydrogenase, nuoA-N	MK + NADH -> MKH2 + NAD + 4 H	0.025	0.003	0.272
mdh/Rv1240	malate dehydrogenase	NAD + MAL <=> NADH + OA	0	NA	NA
lipY/Rv3097c	Probable Triacylglycerol Lipase	TAGcat -> 0.2 HEXADECANOATE + 0.1 OCTADECANOATE + 0.1 9-OCTADECENOATE + 0.1 EICOSANOATE + 0.1 TETRACOSANOATE + 0.1 HEXACOSANOATE + 0.1 PENTADECANOATE + 0.1 NONADECANOATE + DAG	0	NA	NA
glpX/Rv1099c	fructose-	FDP -> F6P + PI	0	NA	NA

	bisphosphatase				
glpK/Rv3696c	Glycerol kinase glpK	GL + ATP -> ADP + GL3P	0	NA	NA
glcB/Rv1837c	malate synthase	ACCOA + GLX -> COA + MAL	0.010	0.007	0.272
gap/Rv1436	glyceraldehyde-3-phosphate dehydrogenase	NAD + PI + G3P <=> NADH + 13PDG	0.013	0.007	0.272
fum/Rv1098c	fumarate hydratase	FUM <=> MAL	0	NA	NA
fba/Rv0363c	fructose-bisphosphate aldolase-fba, fructose-bisphosphate aldolas	F1P -> DHAP + T3 , FDP <=> DHAP + G3P	0	NA	NA
eno/Rv1023	phosphopyruvate hydratase	2PG <=> PEP	0.010	0.007	0.272
ctaB/Rv1451, Rv1456c, ctaE/Rv2193, qcrC/Rv2194, qcrA/Rv2195, qcrB/Rv2196, ctaC/Rv2200c, fixB/Rv3028c, fixA/Rv3029c, ctaD/Rv3043c	aa3-type cytochrome c oxidase, ctaCDE AND cytochrome bc1	0.5 O2 + 2 HEME-FE2 -> 6 H + 2 HEME-FE3	0.019	0.002	0.272
aglA/Rv2471	alpha-glucosidase	MLT -> 2 GLC , SUC -> GLC + FRU	0	NA	NA

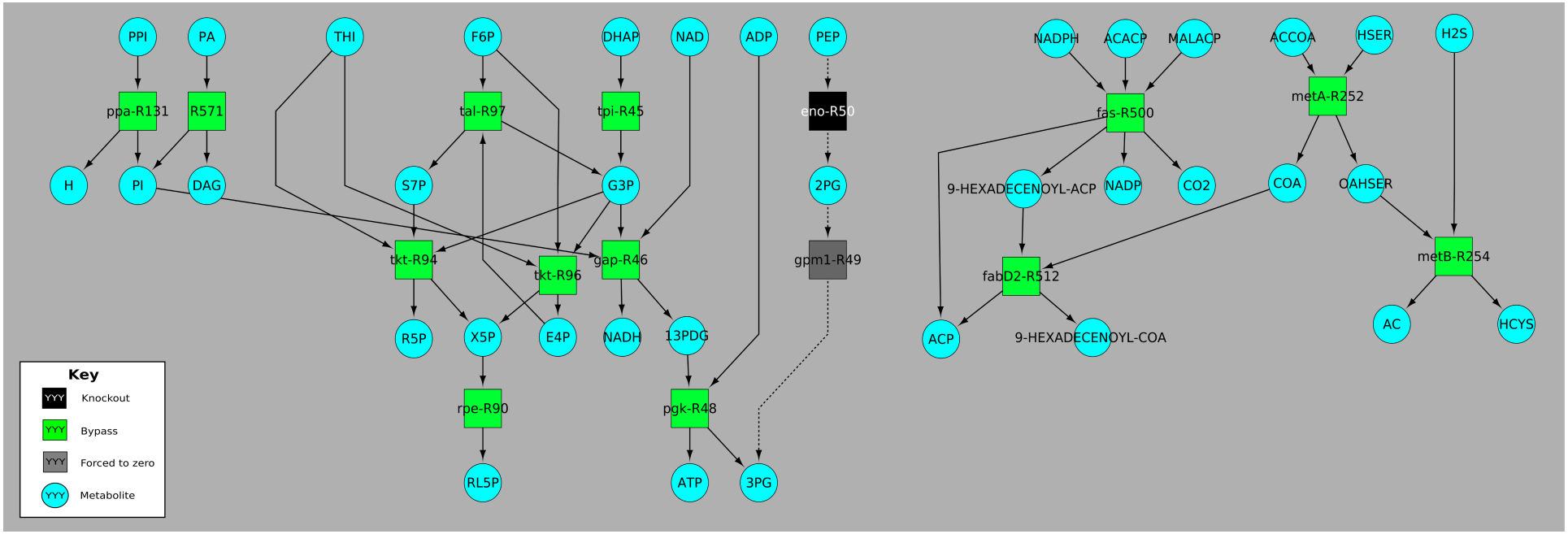

Figure S6: The bypass metabolic network when enolase (eno) is knocked out. This suggests that the knockout compensates for loss of eno by restoring flux to 3PG (3-phosphoglycerate) using the forced positive reaction network on the left. The role of the disconnected network on the right is not clear from this diagram. The analysis of further reactions downstream and upstream of the listed metabolites may be helpful in clarifying this.

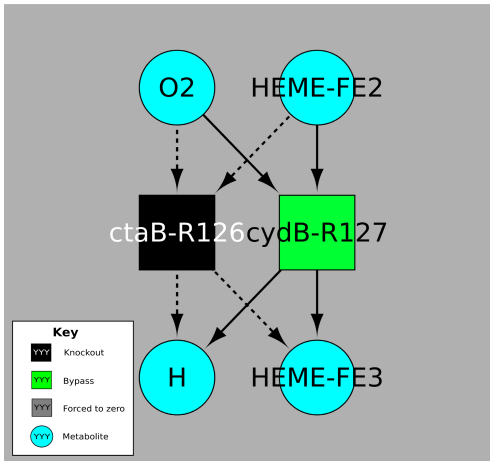

Figure S7: Bypass network for ctaB. Also featured in Fig.10A, shown here for completeness.

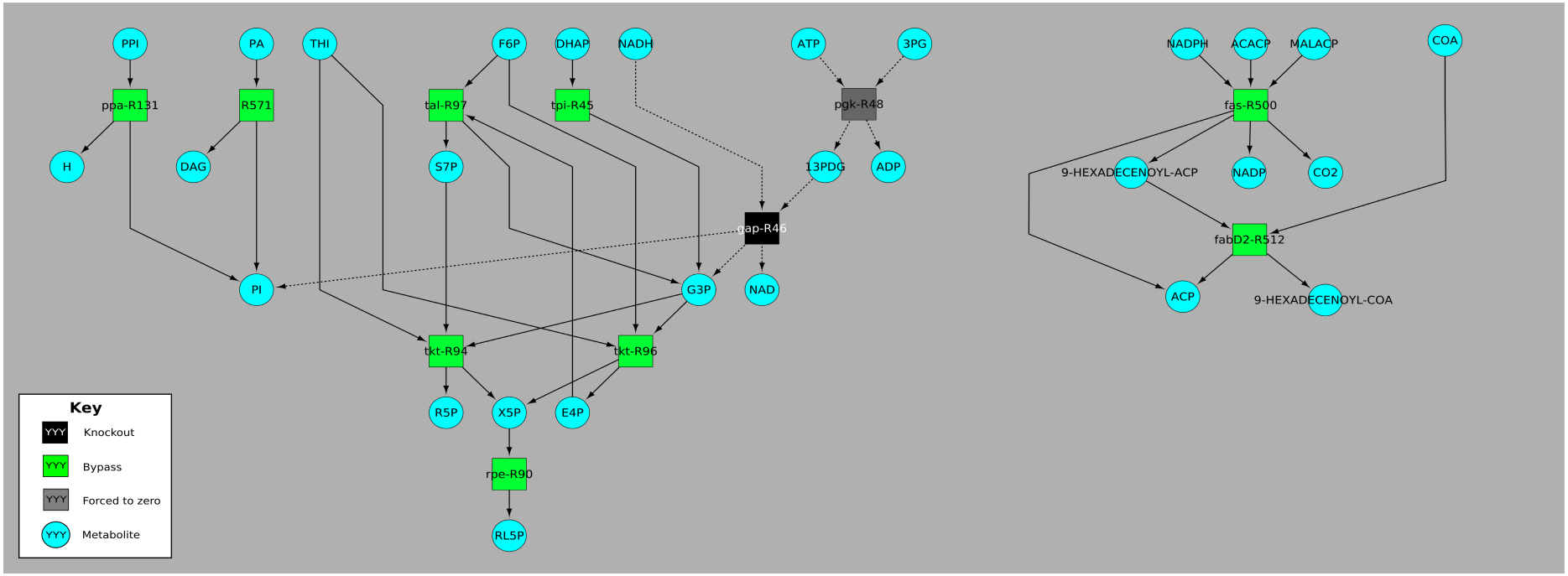

Figure S8: Bypass network for gap.

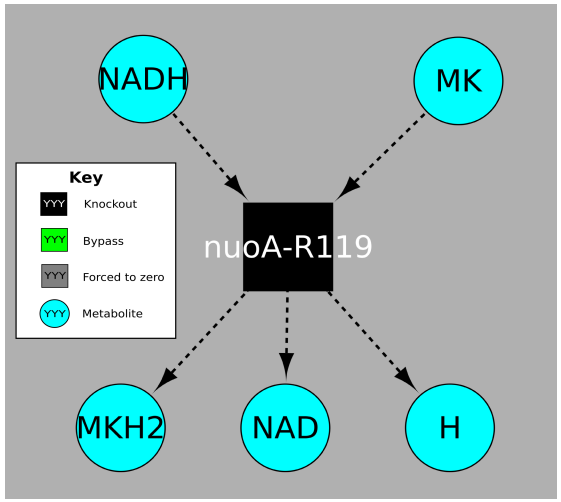

Figure S9: Bypass network for nuoA.

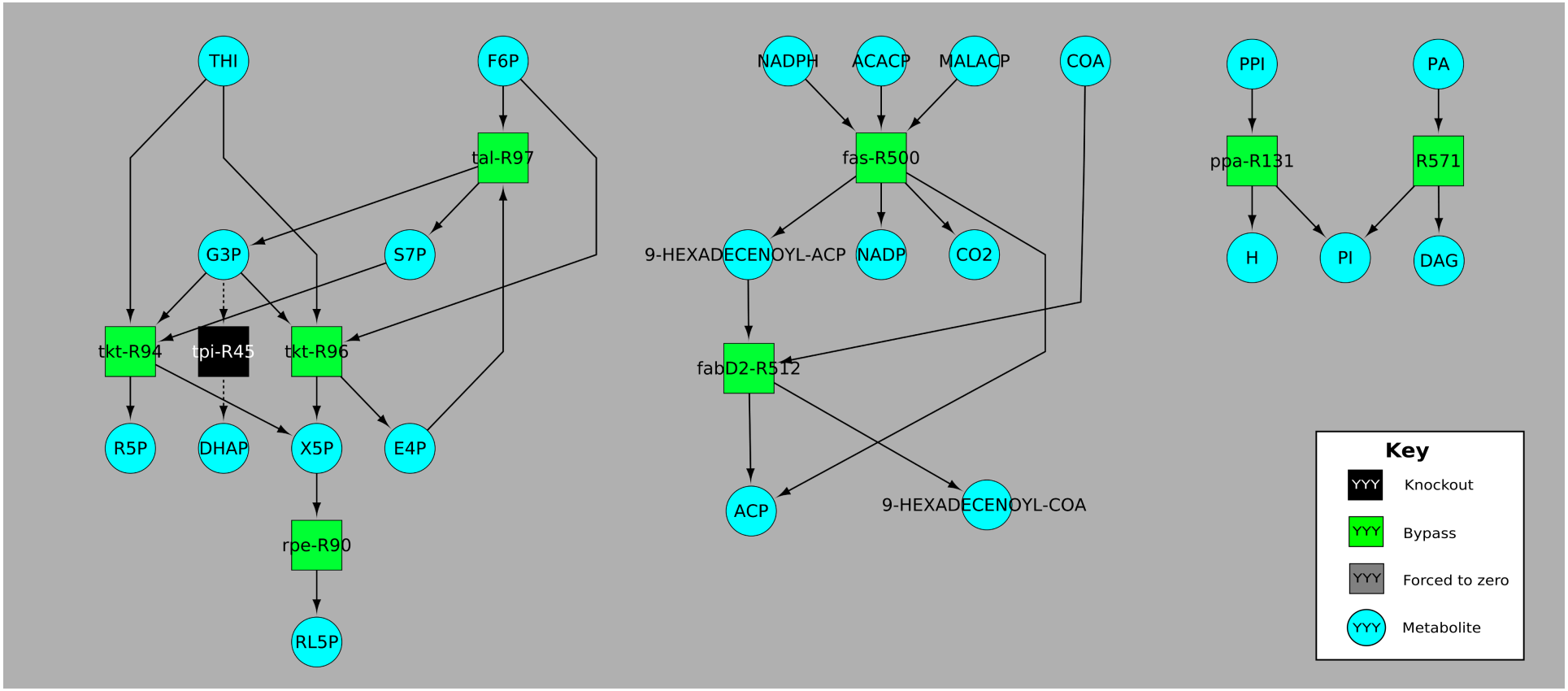

Figure S10: Bypass network for tpi.

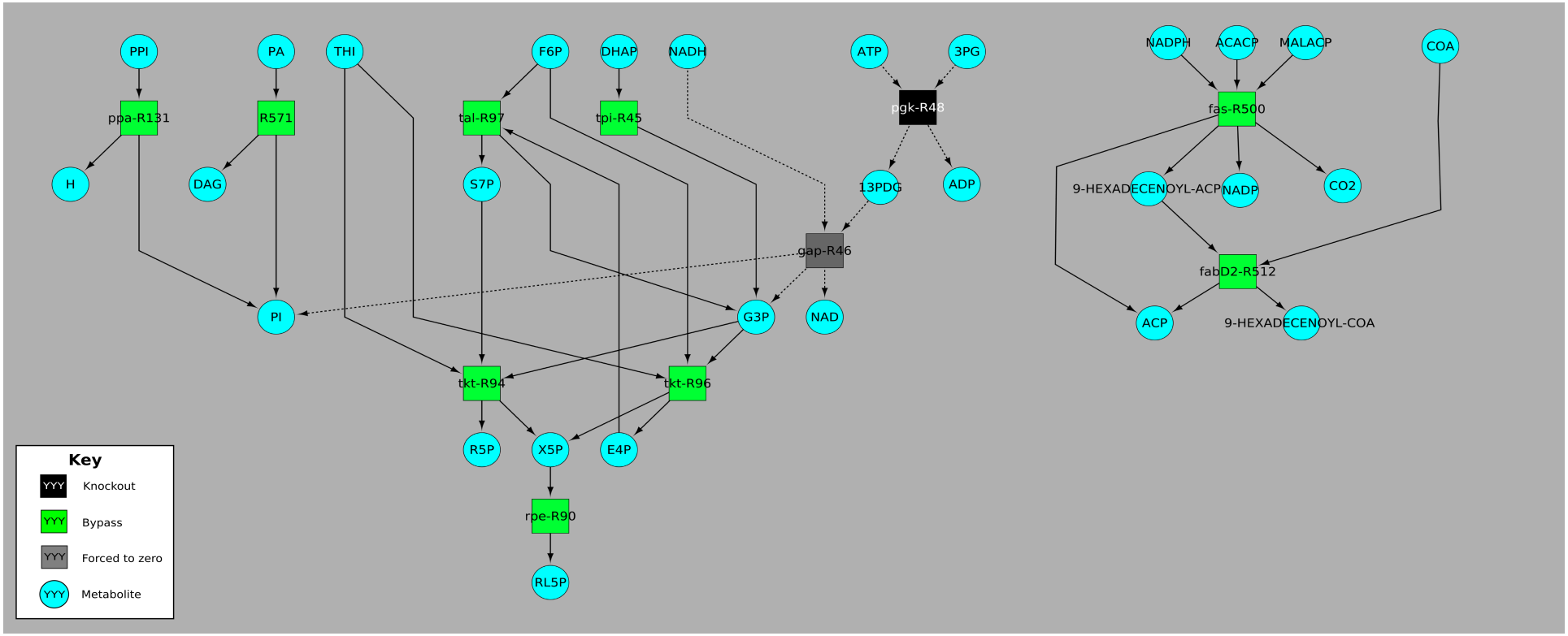

Figure S11: Bypass network for pgk.

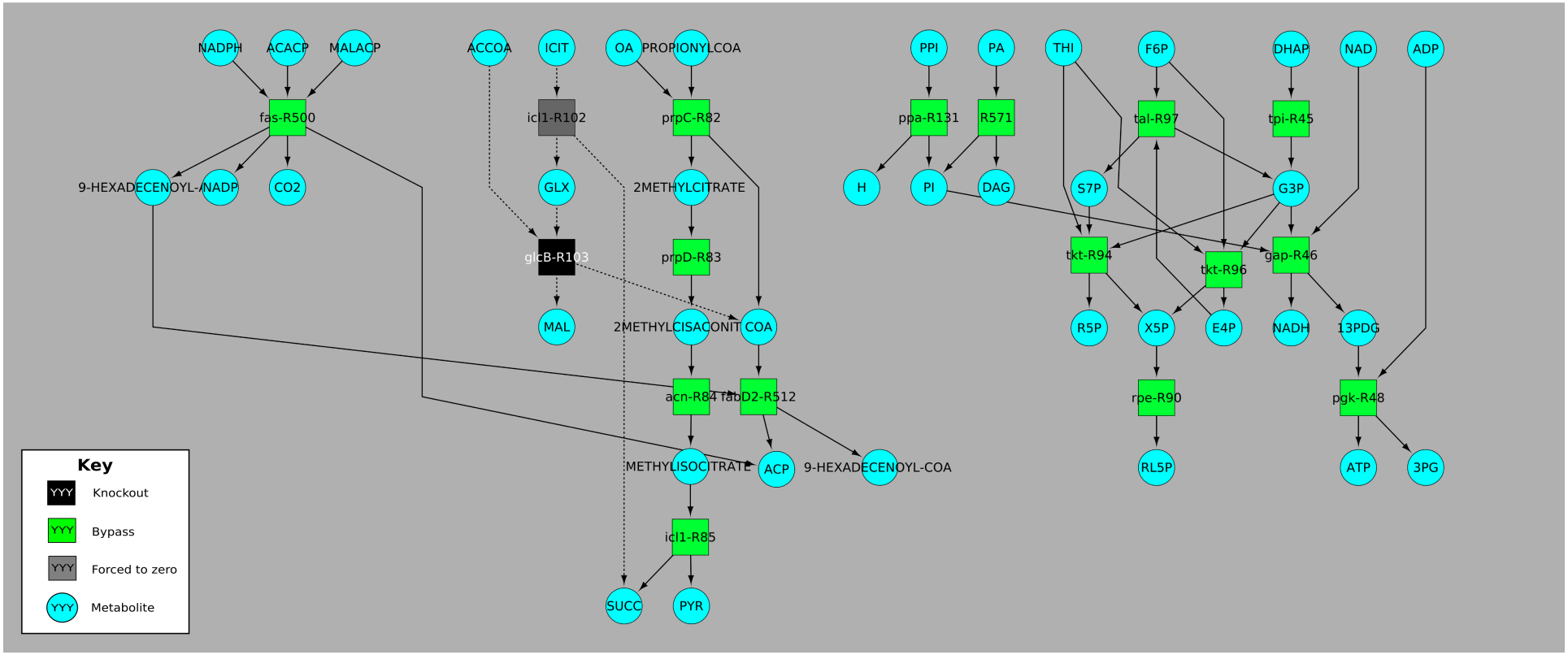

Figure S12: Bypass network for glcB.

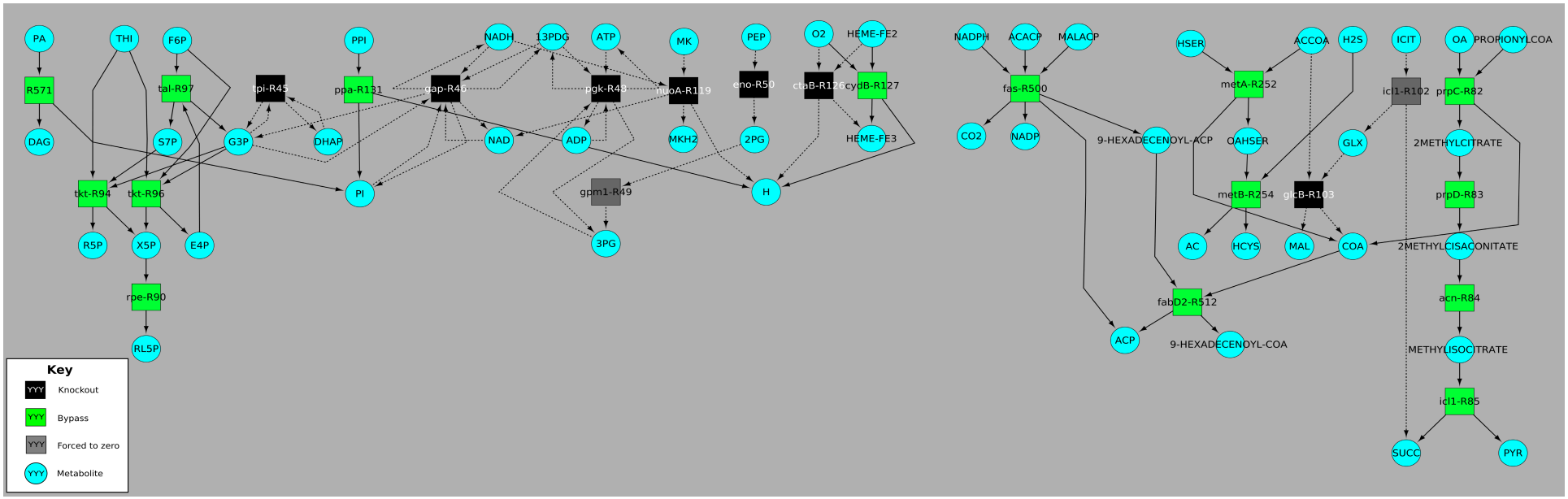

Figure S13: Displayed is a merge of the seven bypass networks featured above. A node is displayed in black if the gene was knocked out in one of the seven networks. A node is grey if it was never a knockout and it was forced to zero in at least one of the seven networks. A node is green if it was required to have positive flux in at least one of the seven mutants and never was knocked out or forced to zero.

References

1. **Lin PL, Coleman T, Carney JP, Lopresti BJ, Tomko J, Fillmore D, Dartois V, Scanga C, Frye LJ, Janssen C, Klein E, Barry CE, 3rd, Flynn JL.** 2013. Radiologic responses in cynomolgous macaques for assessing tuberculosis chemotherapy regimens. Antimicrob Agents Chemother doi:10.1128/AAC.00277-13.
2. **Lin PL, Dartois V, Johnston PJ, Janssen C, Via L, Goodwin MB, Klein E, Barry CE, 3rd, Flynn JL.** 2012. Metronidazole prevents reactivation of latent Mycobacterium tuberculosis infection in macaques. Proc Natl Acad Sci U S A **109:**14188-14193.
3. **Lin PL, Ford CB, Coleman MT, Myers AJ, Gawande R, Ioerger T, Sacchettini J, Fortune SM, Flynn JL.** 2014. Sterilization of granulomas is common in active and latent tuberculosis despite within-host variability in bacterial killing. Nat Med **20:**75-79.
4. **Lin PL, Rodgers M, Smith L, Bigbee M, Myers A, Bigbee C, Chiosea I, Capuano SV, Fuhrman C, Klein E, Flynn JL.** 2009. Quantitative comparison of active and latent tuberculosis in the cynomolgus macaque model. Infect Immun **77:**4631-4642.
5. **Lin PL, Myers A, Smith L, Bigbee C, Bigbee M, Fuhrman C, Grieser H, Chiosea I, Voitenek NN, Capuano SV, Klein E, Flynn JL.** 2010. Tumor necrosis factor neutralization results in disseminated disease in acute and latent Mycobacterium tuberculosis infection with normal granuloma structure in a cynomolgus macaque model. Arthritis Rheum **62:**340-350.
6. **Bean AG, Roach DR, Briscoe H, France MP, Korner H, Sedgwick JD, Britton WJ.** 1999. Structural deficiencies in granuloma formation in TNF gene-targeted mice underlie the heightened susceptibility to aerosol Mycobacterium tuberculosis infection, which is not compensated for by lymphotoxin. J Immunol **162:**3504-3511.
7. **Flynn JL, Chan J, Triebold KJ, Dalton DK, Stewart TA, Bloom BR.** 1993. An essential role for interferon gamma in resistance to Mycobacterium tuberculosis infection. J Exp Med **178:**2249-2254.
8. **Cooper AM, Dalton DK, Stewart TA, Griffin JP, Russell DG, Orme IM.** 1993. Disseminated tuberculosis in interferon gamma gene-disrupted mice. J Exp Med **178:**2243-2247.
9. **O'Garra A, Redford PS, McNab FW, Bloom CI, Wilkinson RJ, Berry MP.** 2013. The immune response in tuberculosis. Annu Rev Immunol **31:**475-527.
10. **Cyktor JC, Carruthers B, Kominsky RA, Beamer GL, Stromberg P, Turner J.** 2013. IL-10 inhibits mature fibrotic granuloma formation during Mycobacterium tuberculosis infection. J Immunol **190:**2778-2790.
11. **Pitt JM, Stavropoulos E, Redford PS, Beebe AM, Bancroft GJ, Young DB, O'Garra A.** 2012. Blockade of IL-10 signaling during bacillus Calmette-Guerin vaccination enhances and sustains Th1, Th17, and innate lymphoid IFN-gamma and IL-17 responses and increases protection to Mycobacterium tuberculosis infection. J Immunol **189:**4079-4087.
12. **Beste DJ, Hooper T, Stewart G, Bonde B, Avignone-Rossa C, Bushell ME, Wheeler P, Klamt S, Kierzek AM, McFadden J.** 2007. GSMN-TB: a web-based genome-scale network model of Mycobacterium tuberculosis metabolism. Genome Biol **8:**R89.
13. **Jamshidi N, Palsson BO.** 2007. Investigating the metabolic capabilities of Mycobacterium tuberculosis H37Rv using the in silico strain iNJ661 and proposing alternative drug targets. BMC Syst Biol **1:**26.
14. **Raman K, Rajagopalan P, Chandra N.** 2005. Flux balance analysis of mycolic acid pathway: targets for anti-tubercular drugs. PLoS Comput Biol **1:**e46.